PROCEEDINGS OF SCIENCE

Collapse of Flow: Probing the Order of the Phase Transition

Horst Stöcker*
FIAS- Frankfurt Institute for Advanced Studies,
Max-von-Laue-Str. 1, 60438 Frankfurt, Germany,
Institut für Theoretische Physik, Johann Wolfgang Goethe - Universität,
Max-von-Laue-Str. 1, 60438 Frankfurt, Germany
Gesellschaft für Schwerionenforschung (GSI),
Planckstr. 1, 64291 Darmstadt
E-mail: stoecker@fias.uni-frankfurt.de

We discuss the present collective flow signals for the phase transition to the quark-gluon plasma (QGP) and the collective flow as a barometer for the equation of state (EoS). We emphasize the importance of the flow excitation function from 1 to 50A GeV: here the hydrodynamic model has predicted the collapse of the v_1-flow at $\sim 10A$ GeV and of the v_2-flow at $\sim 40A$ GeV. In the latter case, this has recently been observed by the NA49 collaboration. Since hadronic rescattering models predict much larger flow than observed at this energy, we interpret this observation as potential evidence for a first order phase transition at high baryon density ρ_B.

The 4rd edition of the International Workshop — The Critical Point and Onset of Deconfinement — July 9-13 2007
Gesellschaft für Schwerionenforschung, Darmstadt, Germany

*Speaker.

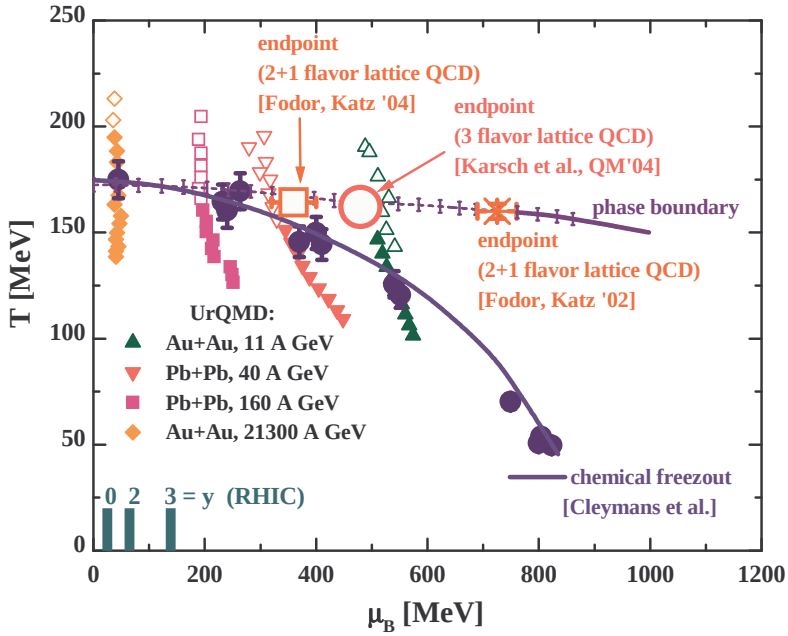

Figure 1: The phase diagram with the critical end point at $\mu_B \approx 400$ MeV, $T \approx 160$ MeV, predicted by Lattice QCD calculations. For different bombarding energies, the time evolution in the $T - \mu_B$–plane of a central cell in UrQMD calculations [10] is depicted. (from Bratkovskaya *et al.*) [8].

1. The QCD phase diagram

The phase diagram predicted by lattice QCD calculations [1, 2] (Fig. 1) shows a cross over for vanishing or small chemical potentials μ_B, but no first-order phase transition to the quark-gluon plasma (QGP). This region may be accessible at full RHIC energy. In contrast, at lower SPS and RHIC energies ($\sqrt{s} \approx 4 - 12A$ GeV) and in the fragmentation region of RHIC, $y \approx 3 - 5$ [3, 4] a first-order phase transition is expected with a critical baryochemical potential of [1, 2] $\mu_B^c \approx 400 \pm 50$ MeV and a critical temperature of $T_c \approx 150 - 160$ MeV. This first-order phase transition is expected to occur at finite strangeness [5].

A comparison of the QCD predictions of the thermodynamic parameters T and μ_B with the results from the UrQMD transport model [6, 7] in the central overlap regime of Au+Au collisions [8] are shown in Figure 1. The 'experimental' chemical freeze-out parameters – determined from fits to the experimental yields – are shown by full dots with errorbars and taken from Ref. [9]. The temperature T and chemical potentials μ_B, denoted by triangular and quadratic symbols (time-ordered in vertical sequence), are taken from UrQMD transport calculations in central Au+Au (Pb+Pb) collisions at RHIC [10] as a function of the reaction time (separated by 1 fm/c steps from top to bottom). Full symbols denote configurations in approximate pressure equilibrium in longitudinal and transverse direction, while open symbols denote nonequilibrium configurations and correspond to T parameters extracted from the transverse momentum distributions.

The transport calculations during the nonequilibrium phase (open symbols) show much higher temperatures (or energy densities) than the 'experimental' chemical freeze-out configurations at all bombarding energies ($\geq 11A$ GeV). These numbers exceed the critical point of (2+1) flavor

lattice QCD calculations by the Bielefeld-Swansea-collaboration [2] (large open circle) and by the Wuppertal-Budapest-collaboration [1] (open square; the star denotes earlier results from [1]). The energy density at μ_c, T_c is of the order of ≈ 1 GeV/fm^3. At RHIC energies, when the temperature drops during the expansion phase of the 'hot fireball' a cross over is expected at midrapidity. Using the statistical model analysis by the BRAHMS collaboration based on measured antibaryon to baryon ratios [11] for different rapidity intervals at RHIC energies, the baryochemical potential μ_B has been obtained. At midrapidity, one observes $\mu_B \simeq 0$, whereas at forward rapidities μ_B increases up to $\mu_B \simeq 130$ MeV at $y = 3$. Thus, only a forward rapidity measurement ($y \approx 4-5$) at RHIC will allow to probe large μ_B. A unique opportunity to reach higher chemical potentials and the first-order phase transition region at midrapidity is offered by the STAR and PHENIX detectors at RHIC in the high-μ-RHIC-running at $\sqrt{s} = 4-12A$ GeV. For first results see Ref. [12]. The International FAIR Facility at GSI will offer a research program fully devoted to this topic in the next decade.

1.1 Flow Effects from Hydrodynamics

Early in the 70th, hydrodynamic flow and shock formation have been proposed [13, 14] as the key mechanism for the creation of hot and dense matter in relativistic heavy-ion collisions [15]. Though, the full three-dimensional hydrodynamical flow problem is much more complicated than the one-dimensional Landau model [16]. The 3-dimensional compression and expansion dynamics yields complex triple differential cross sections which provide quite accurate spectroscopic handles on the EoS. Differential barometers for the properties of compressed, dense matter from SIS to RHIC are the bounce-off, $v_1(p_T)$ (i.e., the strength of the directed flow in the reaction plane), the squeeze-out, $v_2(p_T)$ (the strength of the second moment of the azimuthal particle emission distribution) [13, 14, 17, 18, 19, 20, 21], and the antiflow [17, 18, 19, 20, 21] (third flow component [22, 23]). It has been shown [14, 17, 18, 19, 20, 21] that the disappearance or so-called collapse of flow is a direct result of a first-order phase transition.

To determine these different barometers, several hydrodynamic models [24] have been used in the past, starting with the one-fluid ideal hydrodynamic approach. It is known that this model predicts far too large flow effects so that viscous fluid models have been developed [25, 26, 27] to obtain a better description of the dynamics. In parallel, so-called three-fluid models, which distinguish between projectile, target and the fireball fluid, have been considered [28]. Here viscosity effects do not appear inside the individual fluids, but only between different fluids. One aim is to obtain a reliable, three-dimensional, relativistic three-fluid model including viscosity [26, 27].

Though flow can be described very elegantly in hydrodynamics, one should consider microscopic multicomponent (pre-)hadron transport theory, e.g. models like qMD [29], IQMD [30], UrQMD [6, 7], or HSD [31], to control models for viscous hydrodynamics and to gain background models to subtract interesting non-hadronic effects from data. If hydrodynamics with and without quark matter EoS and hadronic transport models without quark matter – but with strings – are compared to data, can we learn whether quark matter has been formed? What degree of equilibration has been reached? What does the EoS look like? How are the particle properties, self-energies, cross sections changed?

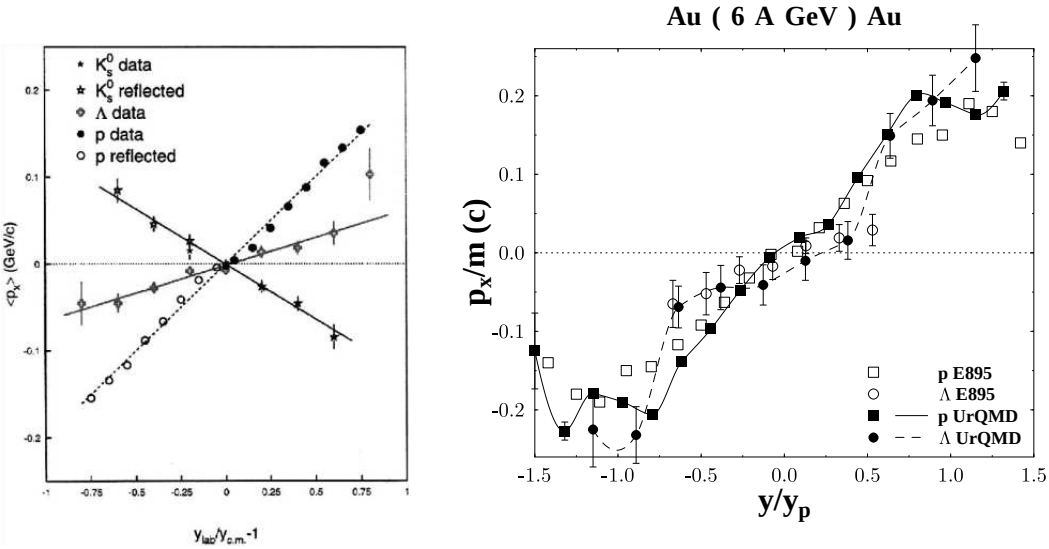

Figure 2: Sideward flow p_x of (left) K, Λ and p's at 6*A* GeV as measured by E895 in semi-central collisions at the AGS and (right) for *p* and Λ compared to UrQMD1.1 calculations for $b < 7$ fm [39] .

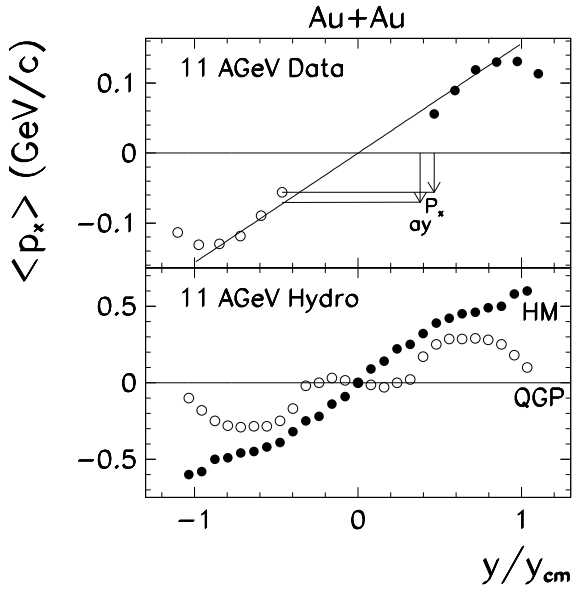

Figure 3: Prediction of the directed flow from ideal hydrodynamics with a QGP phase (open symbols) and from the Quark Gluon String Model without QGP phase (full symbols) [22] .

1.2 Evidence for a first–order phase transition from AGS and SPS

The formation and distribution of many hadronic particles at AGS and SPS is quite well described by microscopic (pre-)hadronic transport models [32]. Additionally, flow data are described reasonably well up to AGS energies [22, 33, 34, 39, 40, 41], if a nuclear potential has been included for the low energy regime.

However, since ideal hydrodynamical calculations predict far too much flow at these energies [25], viscosity effects have to be taken into account. While the directed flow p_x/m measurement of the E895 collaboration shows that the *p* and Λ data are reproduced reasonably well [39, 42],

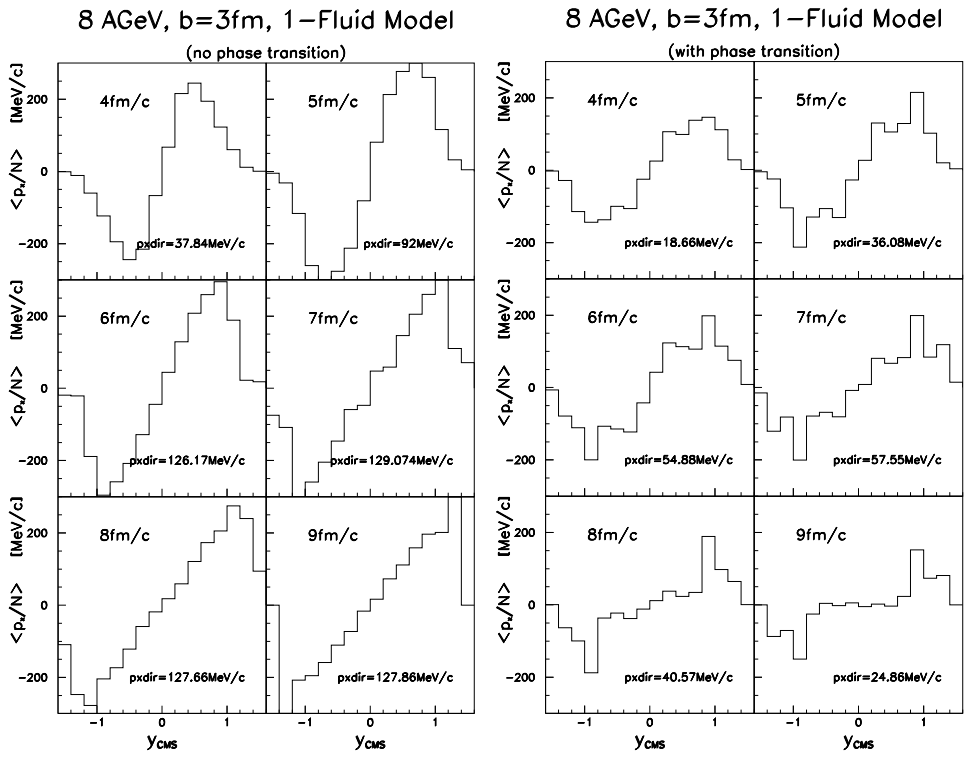

Figure 4: The time evolution of directed flow p_x/N as a function of rapidity for Au+Au collisions at 8A GeV in the one-fluid model for (left) a hadronic EoS without phase transition and (right) an EoS including a first-order phase transition to the QGP [from Brachmann][43].

ideal hydrodynamical calculations yield factors of two higher values for the sideward flow at SIS [25] and AGS.

However, the appearance of a so-called "third flow component" [22] or "antiflow" [43] in central collisions (cf. Fig. 3) is predicted in ideal hydrodynamics, though only if the matter undergoes a first order phase transition to the QGP. It implies that around midrapidity the directed flow, $p_x(y)$, of protons develops a negative slope. Such an exotic "antiflow" (negative slope) wiggle in the proton flow $v_1(y)$ does not appear for a hadronic EoS without QGP phase transition at intermediate energies. For high energies see disussion in References [44, 45]. Just as the microscopic transport theory (Fig. 2 r.h.s.) and as the data (Fig. 2 l.h.s.), the ideal hydrodynamic time evolution of the directed flow, p_x/N, for the purely hadronic EoS (Fig. 4 l.h.s.) does show a clean linear increase of $p_x(y)$. However, it can be seen that for an EoS including a first order phase transition to the QGP (Fig. 4 r.h.s.) that the proton flow $v_1 \sim p_x/p_T$ collapses around midrapidity. This is explained by an antiflow component of protons that develops when the expansion from the plasma sets in [46].

Even negative values of $d(p_x/N)/dy$ calculated from ideal hydrodynamics (Fig. 5) show up between 8 and 20A GeV. An increase up to positive values is predicted with increasing energy. But, the hydro calculations suggest this "softest point collapse" is at $E_{Lab} \approx 8A$ GeV. This predicted minimum of the proton flow has not been verified by the AGS data! However, a collapse of the directed proton flow at $E_{Lab} \approx 30A$ GeV (Fig. 5) is verified by a linear extrapolation of the AGS data.

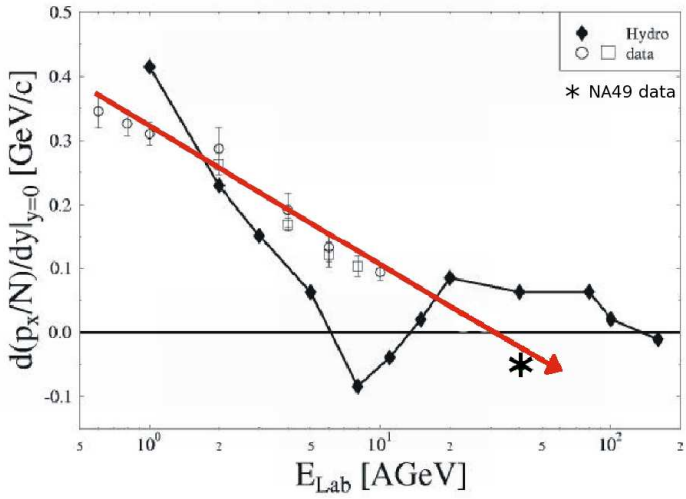

Figure 5: The proton dp_x/dy-slope data measured by SIS and AGS compared to a one-fluid hydrodynamical calculation. A linear extrapolation of the AGS data indicates a collapse of flow at $E_{Lab} \approx 30A$ GeV (see also Ref. [46]). The point at 40*A* GeV is calculated using the NA49 central data (cf. Alt *et al.*) [38].

This prediction has recently been supported by the low energy 40*A* GeV SPS data of the NA49 collaboration [38] (cf. Figs. 6 and 7). In contrast to the AGS data as well as to the UrQMD calculations involving no phase transition (Figs. 6 and 7), the first proton "antiflow" around mid-rapidity is clearly visible in these data.

Thus, a first order phase transition to the baryon rich QGP is most likely observed at bombarding energies of $30-40A$ GeV; e.g. the first order phase transition line in the T-μ_B-diagram has been crossed (cf. Fig. 1). In this energy region, the new FAIR- facility at GSI will operate. It can be expected that the baryon flow collapses and other first order QGP phase transition signals can be studied soon at the lowest SPS energies as well as at fragmentation region $y > 4-5$ for the RHIC and LHC collider energies. At high μ_B, these experiments will enable a detailed study of the first order phase transition as well as of the properties of the baryon rich QGP.

2. More evidence for a first–order phase transition at highest net baryon densities

Microscopic transport models, at SIS energies, reproduce the data on the excitation function of the proton elliptic flow v_2 quite well. The data seem to be described well by a soft, momentum–dependent EoS [47, 48].

Below $\sim 5A$ GeV, the observed proton flow v_2 is smaller than zero, which corresponds to the squeeze-out predicted by hydrodynamics long ago [13, 14, 17, 18, 19, 20, 21].

From the AGS data, a transition from squeeze-out to in-plane flow in the midrapidity region can be seen (Fig. 8). In accord to the transport caluclations (UrQMD calculations in Fig. 8 [39]; for HSD results see [40, 41]), the proton v_2 at $4-5A$ GeV changes its sign. Hadronic transport simulations predict a smooth increase of the flow v_2 at higher energies ($10-160A$ GeV). The

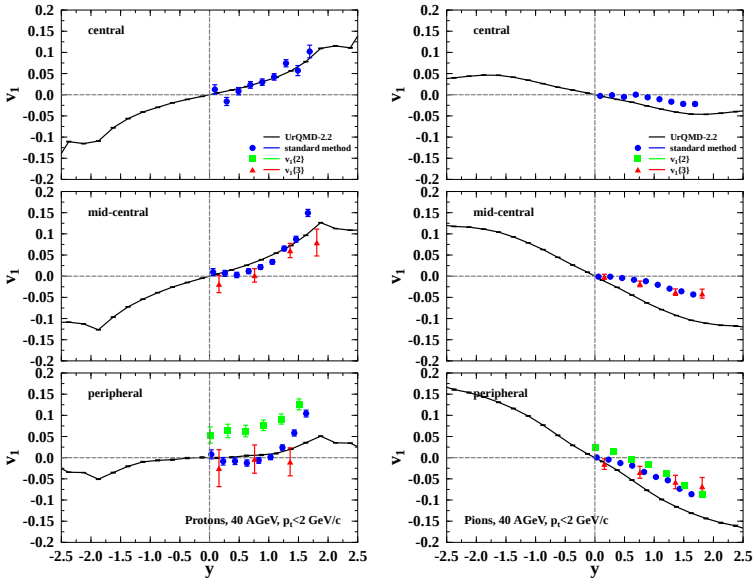

Figure 6: (Color online)Directed flow of protons (left) and pions (right) in Pb+Pb collisions at $E_{\rm lab} = 40A$ GeV with $p_t < 2$ GeV/c. UrQMD calculations are depicted with black lines. The symbols are NA49 data from different analysis methods. The standard method (circles), cumulant method of order 2 (squares) and cumulant method of order 3 (triangles) are depicted. The 12.5% most central collisions are labeled as central, the centrality 12.5% -33.5% as mid-central and 33.5% -100% as peripheral. For the model calculations the corresponding impact parameters of $b \leq 3.4$ fm for central, $b = 5-9$ fm for mid-central and $b = 9-15$ fm for peripheral collisions have been used (from Petersen *et. al.* [49]).

160A GeV data of the NA49 collaboration indicate that this smooth increase proceeds as predicted between AGS and SPS. For midcentral and peripheral protons at 40A GeV (cf. Ref. [39, 42]), UrQMD calculations without phase transition give a considerable 3% v_2 flow.

Contrary, the recent NA49 data at 40A GeV (see Ref. [38, 49] (cf. Figs. 9 and 10) show a sudden collapse of the proton flow for midcentral collisions. At 40A GeV this collapse of v_2 for protons around midrapidity is very pronounced while it is not observed at 160A GeV.

Another evidence for the hypothesis of the observation of a first–order phase transition to QCD is the dramatic collapse of the flow v_1 also observed by NA49 [38], again around 40A GeV, where the collapse of v_2 has been observed. This is the highest energy at which a first-order phase transition can be reached at central rapidities of relativistic heavy-ion collisions (cf. Ref. [1, 2] and Fig. 1). Therefore one may conclude that a first-order phase transition at the highest baryon densities accessible in nature has been seen at these energies in Pb+Pb collisions. As shown in Ref. [50], the elliptic flow clearly distinguishes between a first-order phase transition and a cross over.

3. Summary

Evidence for a first–order phase transition in baryon–rich dense matter is recently presented by the collapse of both, v_1- and v_2-collective flow of protons from the Pb+Pb collisions at 40A GeV

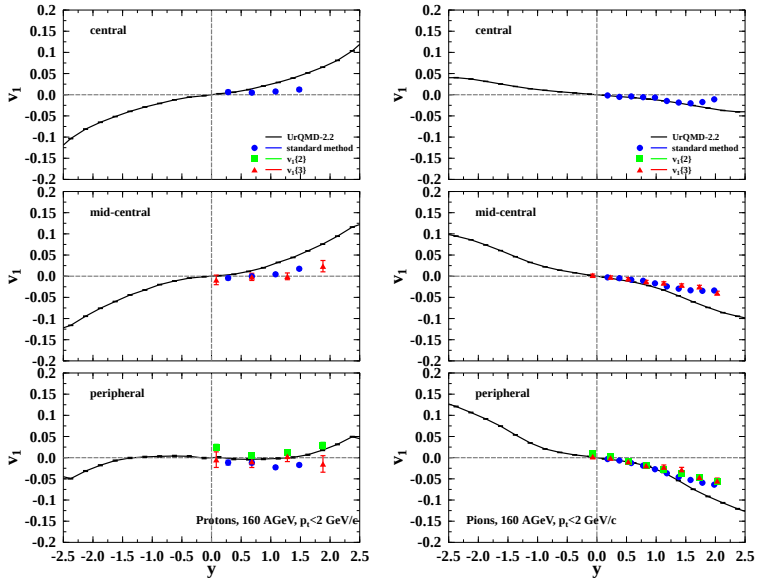

Figure 7: (Color online)Directed flow of protons (left) and pions (right) in Pb+Pb collisions at $E_{\rm lab} = 160A$ GeV with $p_t < 2$ GeV/c. UrQMD calculations are depicted with black lines. The symbols are NA49 data from different analysis methods. The standard method (circles), cumulant method of order 2 (squares) and cumulant method of order 3 (triangles) are depicted. The 12.5% most central collisions are labeled as central, the centrality 12.5% -33.5% as mid-central and 33.5% -100% as peripheral. For the model calculations the corresponding impact parameters of $b \leq 3.4$ fm for central, $b = 5-9$ fm for mid-central and $b = 9-15$ fm for peripheral collisions have been used (from Petersen *et. al.* [49]).

of the NA49 collaboration. It will soon be possible to study the nature of this transition and the properties of the QGP at the high-μ/low energy and at the forward fragmentation region at RHIC and at the future GSI facility FAIR.

This first-order phase transition occurs according to lattice QCD results [1, 2] for chemical potentials above 400 MeV. Since the elliptic flow clearly distinguishes between a first-order phase transition and a cross over [50], the observed collapse of flow, as predicted in Ref. [13, 14], is a clear signal for a first-order phase transition at the highest baryon densities. Calculations from ideal hydrodynamics [51] including additional fluctuations predict an increase of 50% for fluctuations of the flow; however transport models predict an increase by a factor of 2 and 3 [52]. The viscosity coefficient of QGP might experimentally be determined from these fluctuations.

We predict that the collapse of the proton flow analogous to the 40A GeV data will be seen in the second–generation experiments at RHIC and FAIR.

4. Acknowledgements

We like to thank B. Bäuchle, B. Betz, E. Bratkovskaya, M. Bleicher, A. Dumitru, I. Mishustin, K. Paech, H. Petersen, D. Rischke, S. Schramm, G. Zeeb, X. Zhu and D. Zschiesche for discussions.

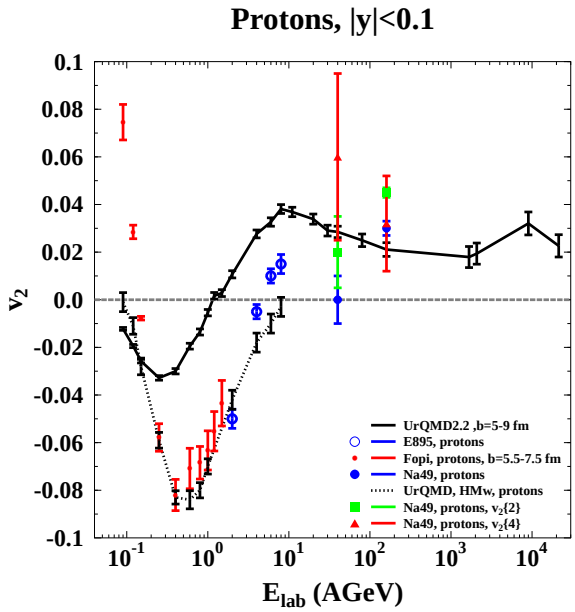

Figure 8: (Color online) The calculated energy excitation function of elliptic flow of protons in Au+Au/Pb+Pb collisions in mid-central collisions (b=5-9 fm) with $|y| < 0.1$(full line). This curve is compared to data from different experiments for mid-central collisions. For E895 [35][36], FOPI [37] and NA49 [38] there is the elliptic flow of protons. The dotted line in the low energy regime depicts UrQMD calculations with included nuclear potential (from Petersen *et. al.* [49]).

References

[1] Z. Fodor and S. D. Katz, JHEP **0203** (2002) 014; JHEP **0404** (2004) 050.

[2] F. Karsch, J. Phys. G **30** (2004) S887; F. Karsch,hep-ph/0701210.

[3] R. Anishetty, Peter Koehler, and Larry D. McLerran, Phys. Rev. **D 22** (1980) 2793.

[4] S. Date, M. Gyulassy, and H. Sumiyoshi, Phys. Rev. **D 32** (1985) 619.

[5] C. Greiner, P. Koch, and H. Stöcker, Phys. Rev. Lett. **58** (1987) 1825; C. Greiner, D. H. Rischke, H. Stöcker, and P. Koch, Phys. Rev. D **38** (1988) 2797.

[6] S. A. Bass *et al.*, Prog. Part. Nucl. Phys. **41** (1998) 255 [Prog. Part. Nucl. Phys. **41** (1998) 225].

[7] M. Bleicher *et al.*, J. Phys. G **25** (1999) 1859.

[8] E. L. Bratkovskaya *et al.*, Phys. Rev. C **69** (2004) 054907.

[9] J. Cleymans and K. Redlich, Phys. Rev. **C60** (1999) 054908.

[10] L. V. Bravina *et al.*, Phys. Rev. **C 60** (1999) 024904; Nucl. Phys. **A 698** (2002) 383.

[11] I. G. Bearden *et al.*, Phys. Rev. Lett. **90** (2003) 102301.

[12] D. Roehrich [for the BRAHMS Collaboration], see this proceedings.

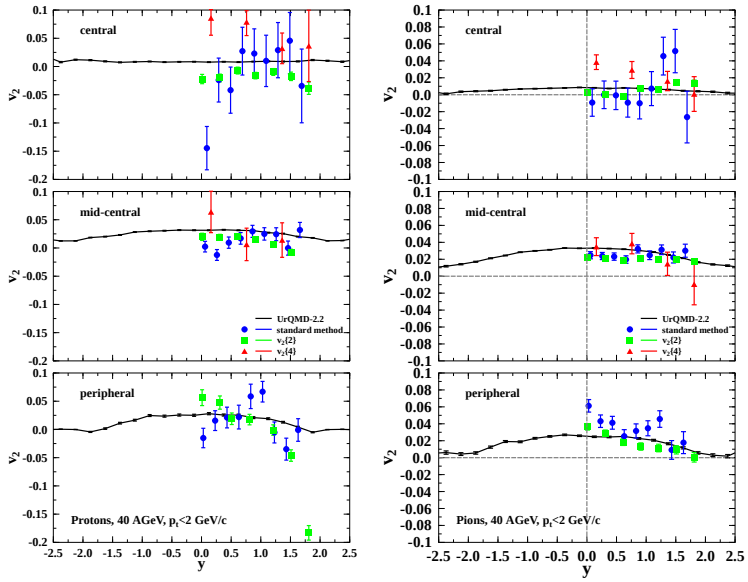

Figure 9: (Color online)Elliptic flow of protons (left) and pions (right) in Pb+Pb collisions at $E_{\rm lab} = 40A$ GeV with $p_t < 2$ GeV/c. UrQMD calculations are depicted with black lines. The symbols are NA49 data from different analysis methods. The standard method (circles), cumulant method of order 2 (squares) and cumulant method of order 3 (triangles) are depicted. The 12.5% most central collisions are labeled as central, the centrality 12.5% -33.5% as mid-central and 33.5% -100% as peripheral. For the model calculations the corresponding impact parameters of $b \leq 3.4$ fm for central, $b = 5-9$ fm for mid-central and $b = 9-15$ fm for peripheral collisions have been used (from Petersen *et. al.* [49]).

[13] J. Hofmann, H. Stöcker, W. Scheid, and W. Greiner, Report of the Int. Workshop on BeV/Nucleon Collisions of Heavy Ions: How and Why, Bear Mountain, New York, Nov. 29 - Dec. 1, 1974 (BNL-AUI 1975).

[14] J. Hofmann, H. Stöcker, U. W. Heinz, W. Scheid, and W. Greiner, Phys. Rev. Lett. **36** (1976) 88.

[15] R. A. Lacey and A. Taranenko, PoS C **FRNC2006** (2006) 021.

[16] L.D. Landau and E.M. Lifshitz, *Fluid Mechanics*, Pergamon Press, New York, 1959.

[17] H. Stöcker, J. Hofmann, J. A. Maruhn, and W. Greiner, Prog. Part. Nucl. Phys. **4** (1980) 133.

[18] H. Stöcker, J. A. Maruhn, and W. Greiner, Phys. Rev. Lett. **44** (1980) 725.

[19] H. Stöcker *et al.*, Phys. Rev. Lett. **47** (1981) 1807.

[20] H. Stöcker *et al.*, Phys. Rev. **C 25** (1982) 1873.

[21] H. Stöcker and W. Greiner. Phys. Rept. **137** (1986) 277.

[22] L. P. Csernai and D. Röhrich, Phys. Lett. **B 458** (1999) 454.

[23] L. P. Csernai *et al.*, hep-ph/0401005.

[24] D. H. Rischke, Y. Pürsün, J. A. Maruhn, H. Stöcker, and W. Greiner, Heavy Ion Phys. **1** (1995) 309.

[25] W. Schmidt *et al.*, Phys. Rev. **C 47** (1993) 2782.

[26] A. Muronga, Heavy Ion Phys. **15** (2002) 337.

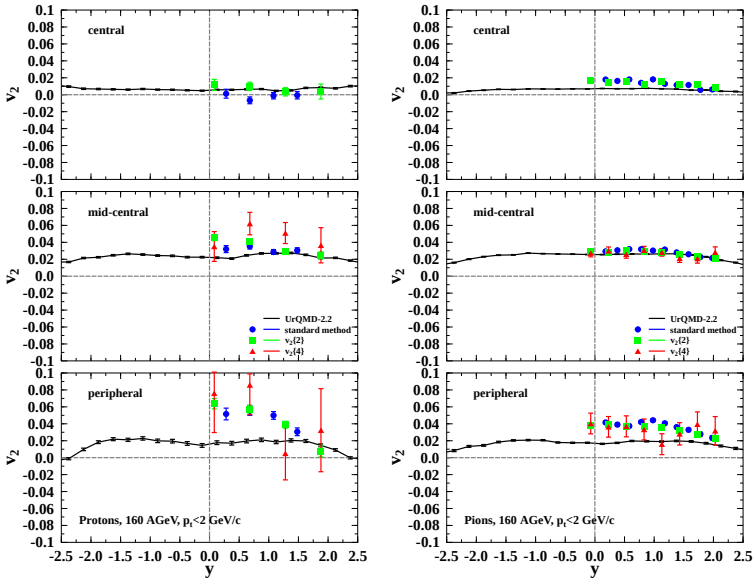

Figure 10: (Color online)Elliptic flow of protons (left) and pions (right) in Pb+Pb collisions at $E_{\rm lab} = 160A$ GeV with $p_t < 2$ GeV/c. UrQMD calculations are depicted with black lines. The symbols are NA49 data from different analysis methods. The standard method (circles), cumulant method of order 2 (squares) and cumulant method of order 3 (triangles) are depicted. The 12.5% most central collisions are labeled as central, the centrality 12.5% -33.5% as mid-central and 33.5% -100% as peripheral. For the model calculations the corresponding impact parameters of $b \leq 3.4$ fm for central, $b = 5-9$ fm for mid-central and $b = 9-15$ fm for peripheral collisions have been used (from Petersen *et. al.* [49]).

[27] A. Muronga, Phys. Rev. **C 69** (2004) 034903.

[28] J. Brachmann *et al.*, Nucl. Phys. **A 619** (1997) 391.

[29] M. Hofmann *et al.*, nucl-th/9908031.

[30] C. Hartnack *et al.*, Nucl. Phys. **A 495** (1989) 303c.

[31] W. Cassing and E. L. Bratkovskaya, Phys. Rept. **308** (1999) 65.

[32] H. Weber, E. L. Bratkovskaya, W. Cassing, and H. Stöcker, Phys. Rev. **C 67** (2003) 014904.

[33] A. Andronic *et al.*, Phys. Rev. **C 67** (2003) 034907.

[34] A. Andronic *et al.*, Phys. Rev. **C 64** (2001) 041604.

[35] C. Pinkenburg *et al.* [E895 Collaboration], *Prepared for Centennial Celebration and Meeting of the American Physical Society (Combining Annual APS General Meeting and the Joint Meeting of the APS and the AAPT), Atlanta, Georgia, 20-26 Mar 1999*

[36] P. Chung *et al.* [E895 Collaboration], Phys. Rev. C **66** (2002) 021901.

[37] A. Andronic *et al.* [FOPI Collaboration], Phys. Lett. B **612** (2005) 173.

[38] C. Alt *et al.*, Phys. Rev. **C 68** (2003) 034903.

[39] S. Soff, S. A. Bass, M. Bleicher, H. Stöcker, and W. Greiner, nucl-th/9903061.

[40] P. K. Sahu and W. Cassing, Nucl. Phys. **A 672** (2000) 376.

[41] P. K. Sahu and W. Cassing, Nucl. Phys. **A 712** (2002) 357.

[42] H. Stöcker, Nucl. Phys. **A 750** (2005) 121.

[43] J. Brachmann, PhD thesis, J. W. Goethe - Universität Frankfurt am Main, 2000.

[44] R. J. M. Snellings, H. Sorge, S. A. Voloshin, F. Q. Wang and N. Xu, Phys. Rev. Lett. **84** (2000) 2803.

[45] M. Bleicher and H. Stoecker, Phys. Lett. B **526** (2002) 309.

[46] J. Brachmann *et al.*, Phys. Rev. **C 61** (2000) 024909.

[47] A. Andronic *et al.*, Nucl. Phys. **A 679** (2001) 765.

[48] A. Andronic, Nucl. Phys. **A 661** (1999) 333.

[49] H. Petersen, Q. Li, X. Zhu and M. Bleicher, Phys. Rev. C **74**, (2006) 064908.

[50] K. Paech, H. Stöcker, and A. Dumitru, Phys. Rev. **C 68** (2003) 044907; Phys. Rev. **C 62** (2000) 064611.

[51] R. Andrade, F. Grassi, Y. Hama, T. Kodama and O. . J. Socolowski, Phys. Rev. Lett. **97** (2006) 202302.

[52] S. Vogel, G. Torrieri and M. Bleicher, arXiv:nucl-th/0703031.